***Conflict of Interest**

Properties and structural behavior of concrete containing fine sand contaminated with light crude oil

Rajab Abousnina[ab*], Allan Manalo[a], Weena Lokuge[a], and Khalifa Saif Al-Jabri[b]

There is no conflict of interest

Tables

Table 1: Sieve analysis of coarse aggregates

Sieve size	*% Weight retain*	*Cumulative %*	*% Passing*
19 mm	0	0	100
9.5 mm	4.19	4.19	95.81
4.75 mm	91.34	95.53	4.47
2.36 mm	3.53	99.06	0.94
1.18 mm	0.52	99.58	0.42
600 µm	0.11	99.69	0.31
300 µm	0.06	99.75	0.25
150 µm	0.06	99.81	0.19
75 µm	0.12	99.93	0.07
Pan	0.07	100	0

Table 2: Comparison between light crude oil and Fork w2.5 Motorcycle oil

Specifications	Light crude oil	Fork w2.5 Motorcycle oils	Ref.
Density (kg/L)	0.825	0.827	
Viscosity (mm^2/s)	5.96	6.74	[23, 24]
Temperature (°C)	40	40	

Table 3: Tests conducted and specimen's details

Type of test	***Crude oil content %***	***Specimen size (mm)***	***Number of tests***	***Test time days***
Compressive strength	0,1,2,6,10 and 20	100 ×200	18	28
Tensile strength	0,1,2,6,10 and 20	100 ×200	18	28
Bond slip	0,1,2,6,10 and 20	150 x 150 x 300	18	28
Beam	0 and 6	100 x 250 x 1400	2	28

Table 4 ANOVA results for main and interaction effects

Source	*Sum of squares*	*Degree of freedom*	*Mean squares*	*F-statistics*	*p-values*
Light crude oil	934.217	5	186.8	326.5	2.19×10^{-12}

Table 5: shows four theoretical bond strength data calculated from the four different equations.

Crude oil content %	*Bond stress (Mpa)*	*Wu and Zhao Model [43]*	*Eligehuasen et al.Model [45]*	*Esfahani et al. Model [46]*	*Harajli and Ahmad Model [42]*
		Bond strength			
0	7.72	7.06	6.45	9.67	8.05
1	8.05	7.21	6.58	9.86	8.22
2	7.59	6.67	6.09	9.13	7.61
6	7.41	6.09	5.56	8.33	6.94
10	5.15	5.30	4.84	7.25	6.04
20	1.98	3.11	2.84	4.25	3.54

Figure
Click here to download Figure: Figures.docx

Figures

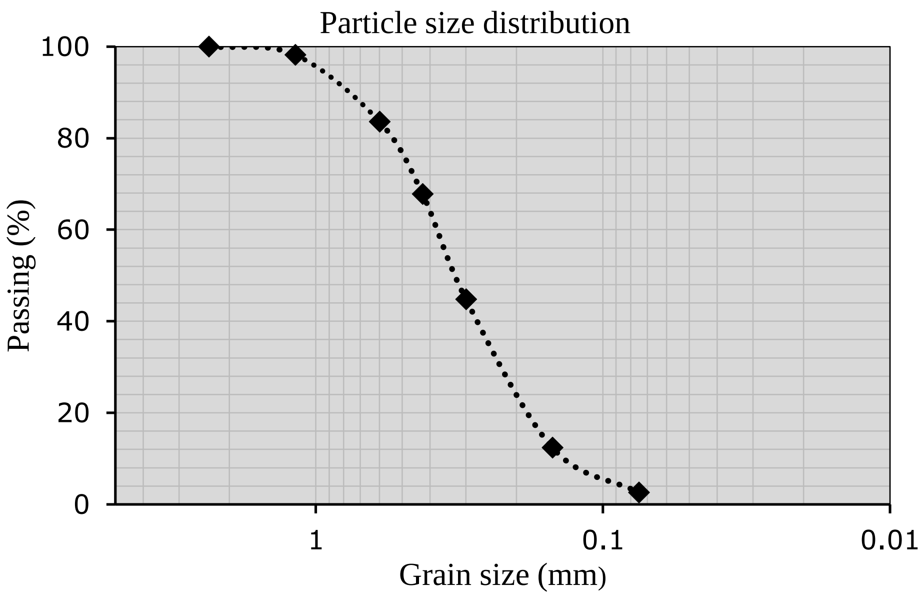

Figure 1: Particle size distribution curve of the sand

Figure 2 Contaminated sand with different percentages of oil (0%-20%)

Figure 3: Bond-slip specimens

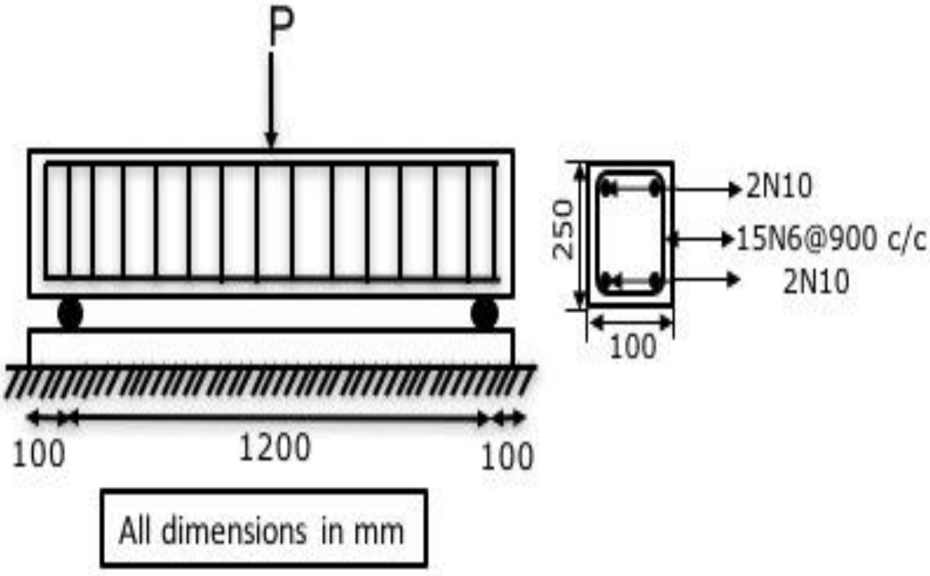

Figure 4: Beam reinforcement details

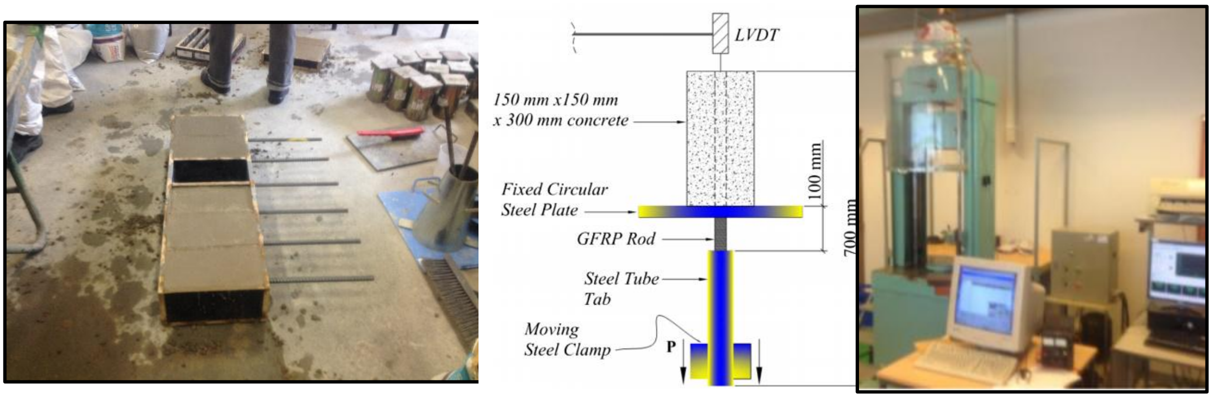

Figure 5: Direct pull-out test (ACI 440.3R-04)

Figure 6: SANS testing machine

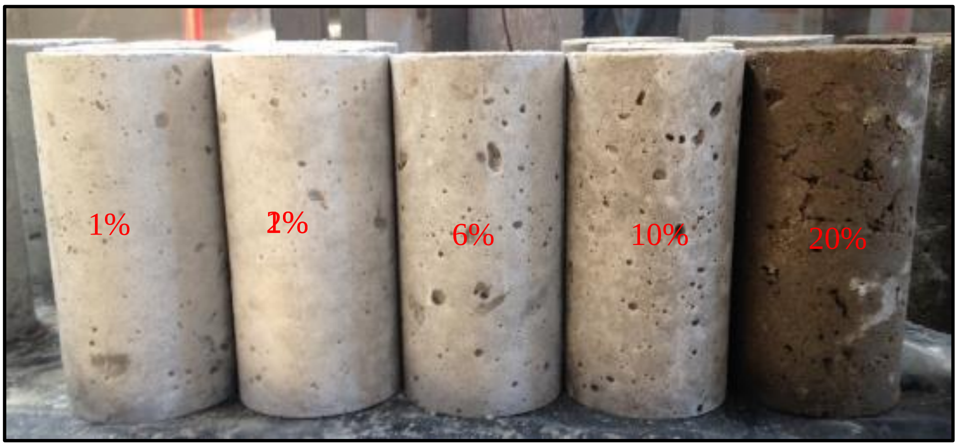

Figure 7 Surface voids of concrete with different levels of crude oil contamination

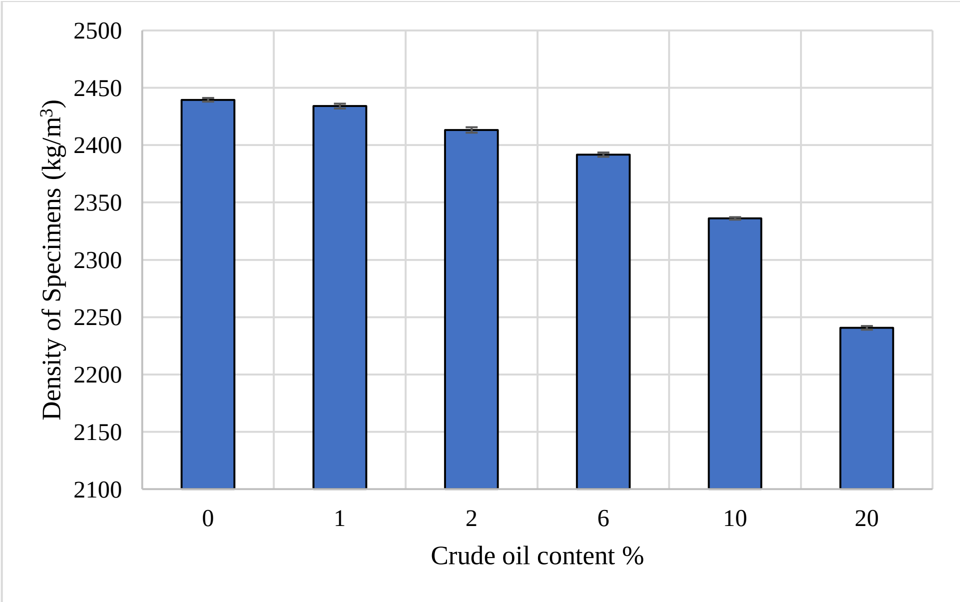

Figure 8 Shows the Density of specimens with varied oil content



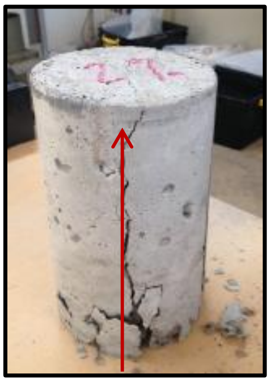

Splitting with fracture conically

Splitting failure

0% 1% 2%


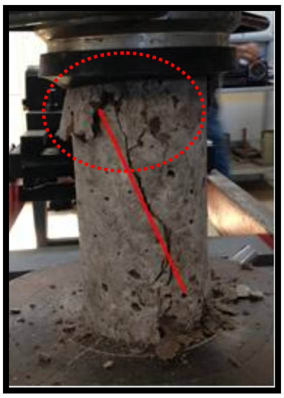
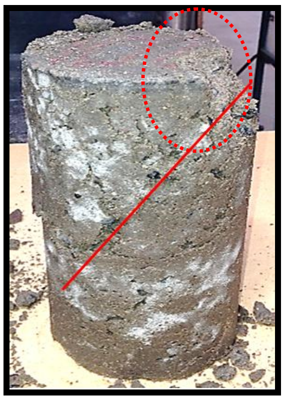

Splitting failure

(Shear failure) with fracture conically

6% 10% 20%

Figure 9 Failure modes of specimens containing different crude oil content. (splitting shear failures with and without fracture)

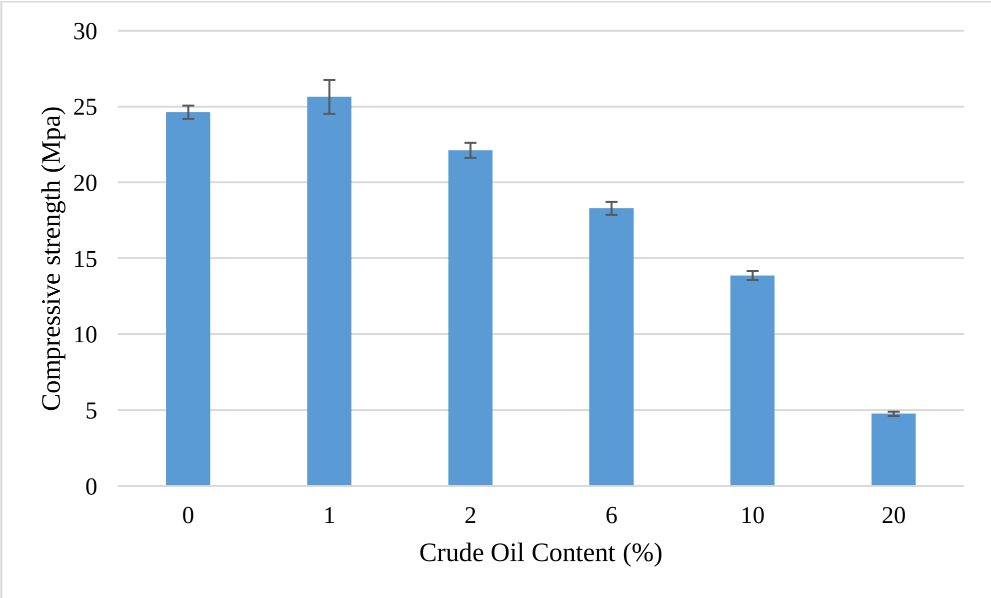

Figure 10 Average compressive strength of specimens with different crude oil content

State		Total saturation	Crude oil content (%)
Uncontaminated aggregate	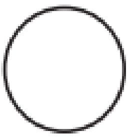	None	 0%
Aggregate partially coated by crude oil	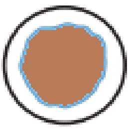	Less than potential absorption	 0.5%-2%
Aggregate coated by crude oil	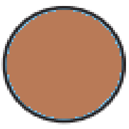	Equal to potential absorption	 4%-6%

Aggregate saturated by crude oil "Saturation status"

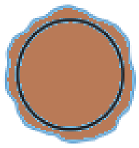

Greater than absorption

10%-20%

Figure 11 Moisture conditions of aggregate (sand, coarse) compared to that observed at a high level of crude oil content (10% and 20%)

(a) 0% (average pore diameter: 454μm)

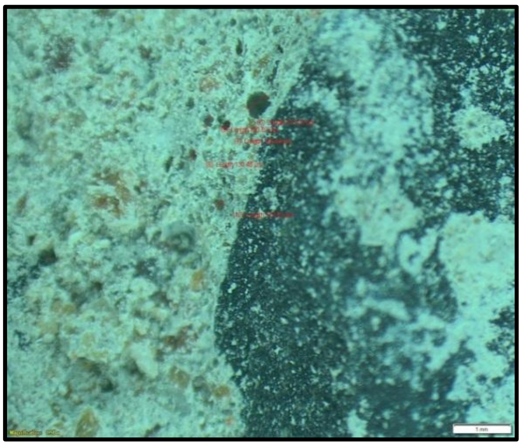

(b) 1% (average pore diameter: 368μm)

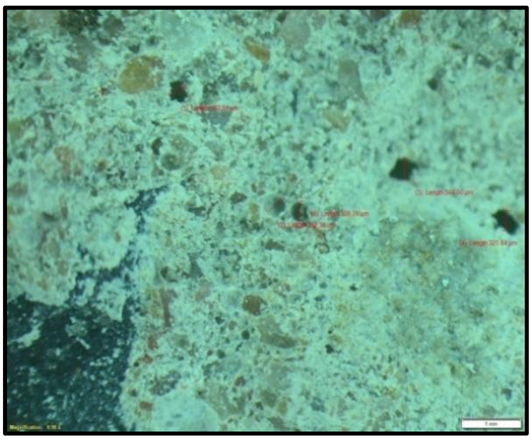

(c) 2% (average pore diameter: 446μm)

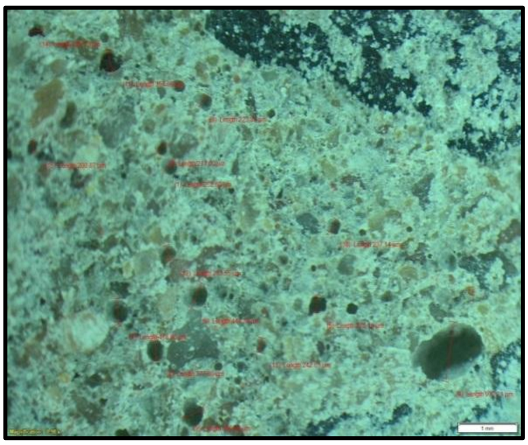

(d) 6% (average pore diameter: 500μm)

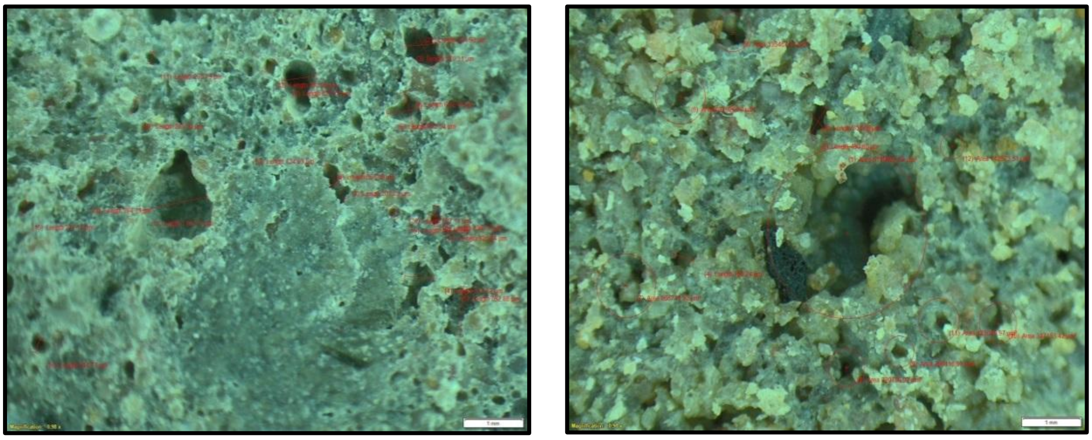

(e)10% (average pore diameter: 720µm) (f) 20% (average pore diameter: 877.95µm)

Figure 12 Pore size diameter of concrete with light crude oil contamination

Oil content (%)	a) Surface of the specimens	b) Microscopic images	c) SEM images
0		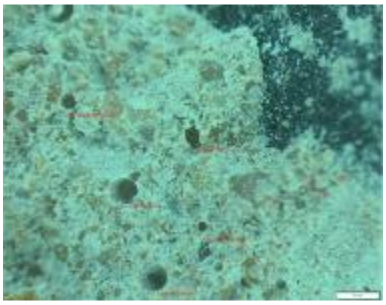	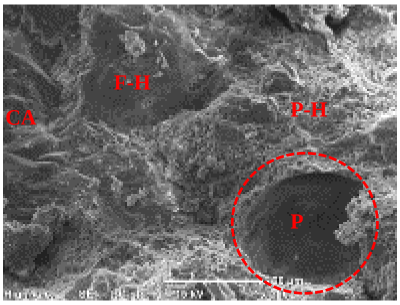
1		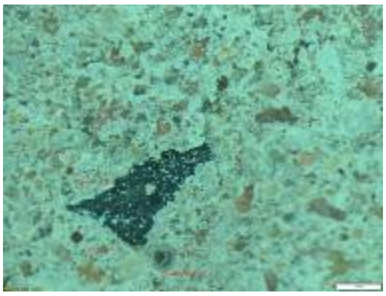	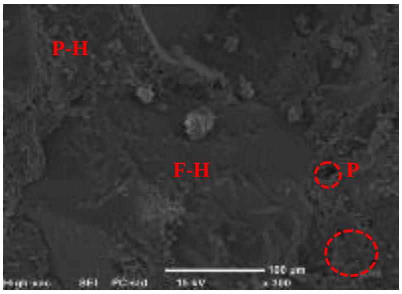
2	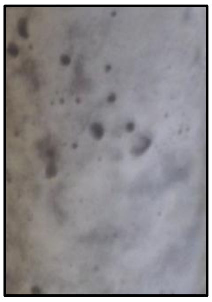	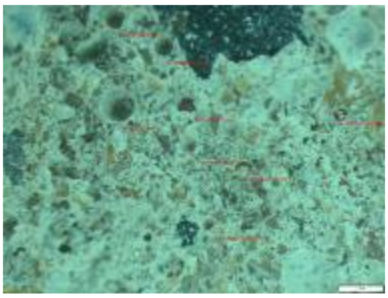	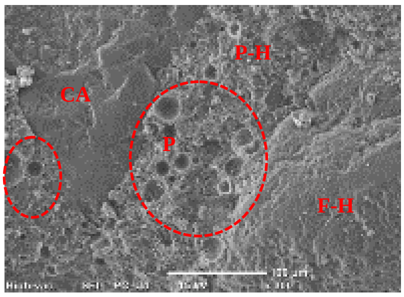

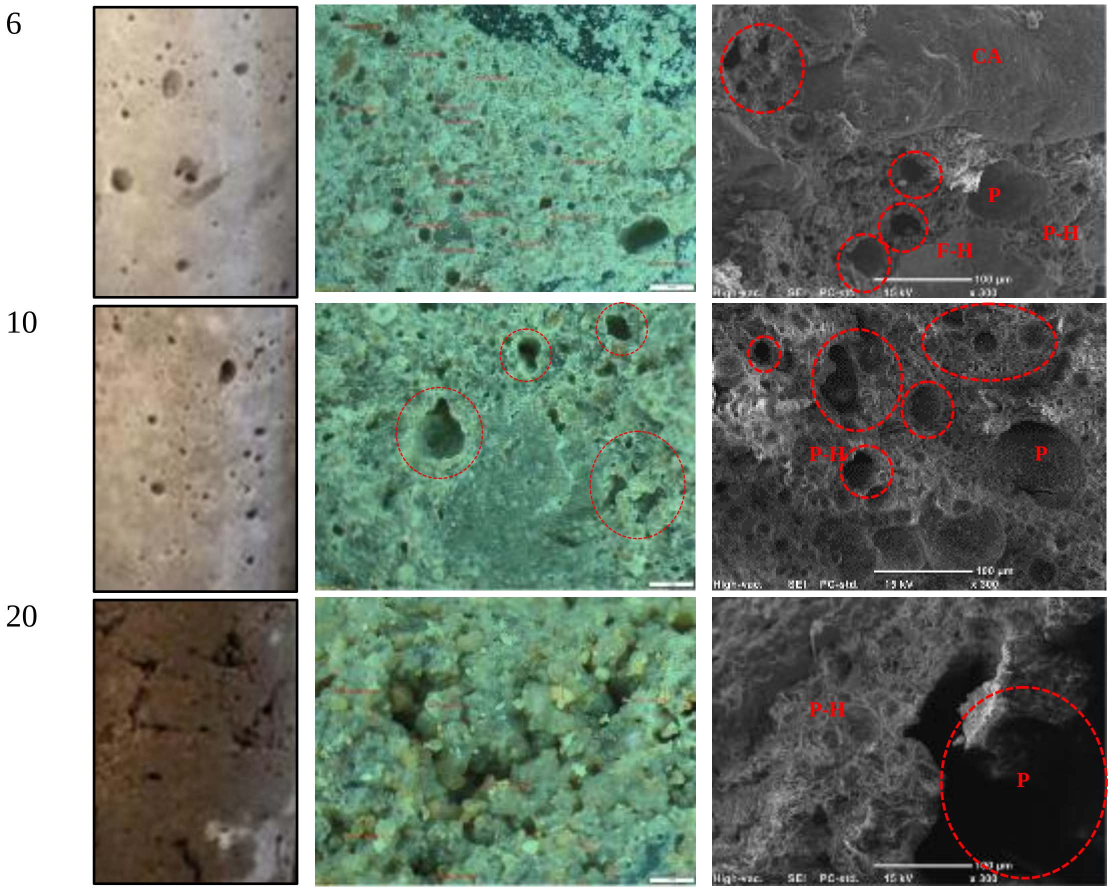

Figure 13 Porosity of the specimens with different crude oil content through visual observation, microscopic images and SEM

Crude oil 0%

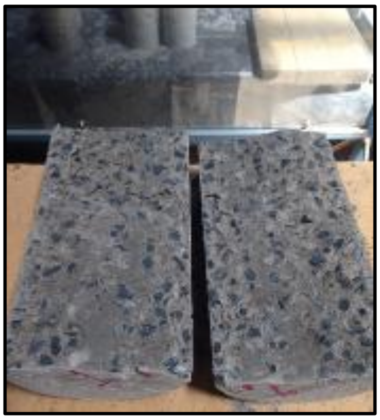

Crude oil 1%

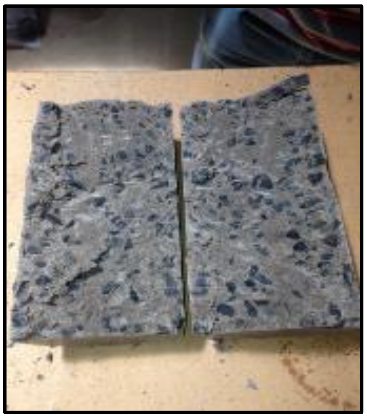

Crude oil 2%

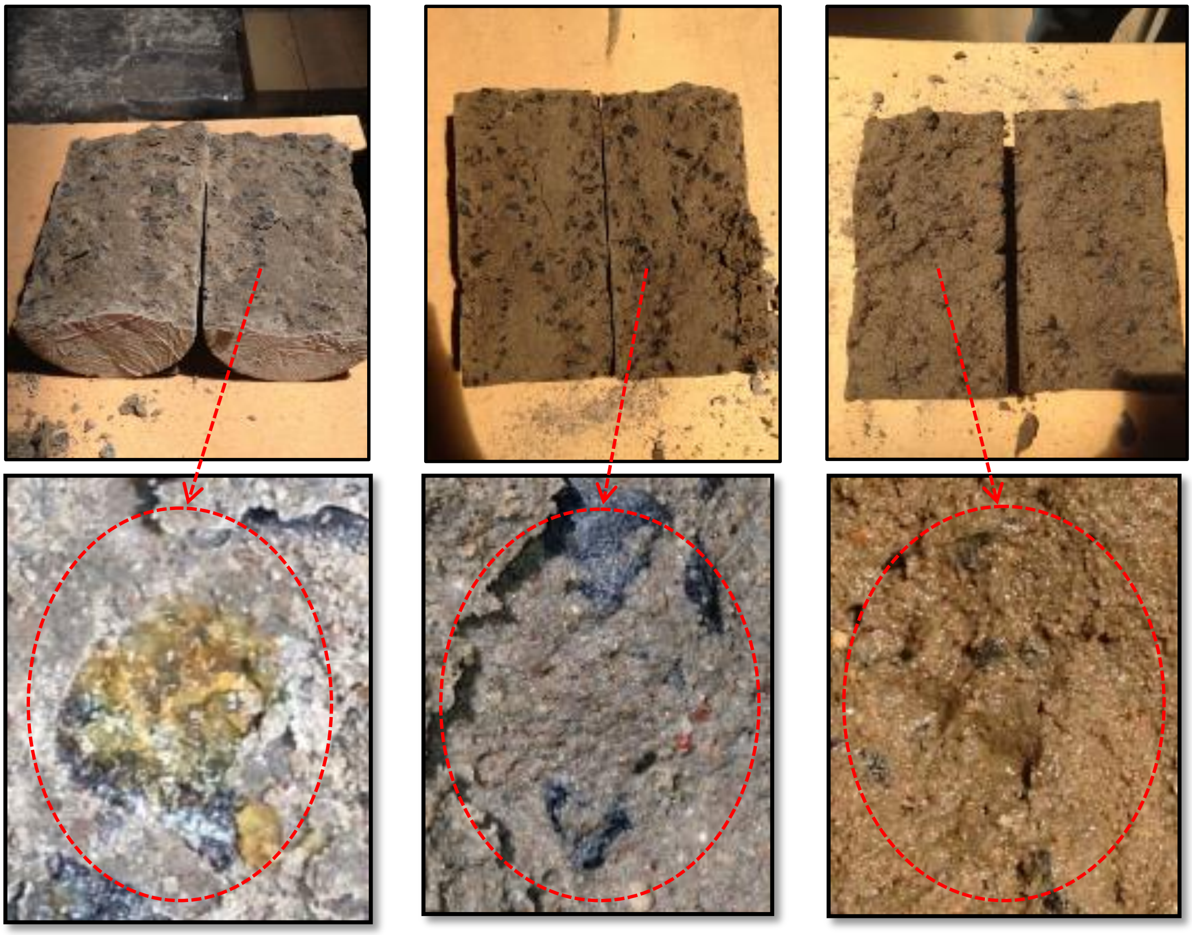

Crude oil 6% Crude oil 10% Crude oil 20%

Figure 14 Splitting tensile failure modes of concrete with different crude oil content

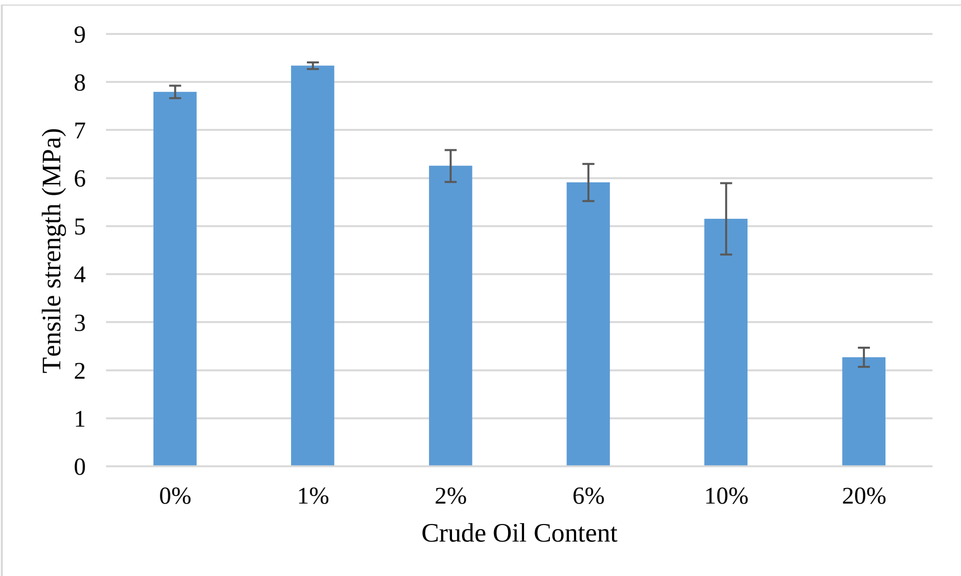

Figure 15 Splitting tensile strength test results of oil contaminated concrete

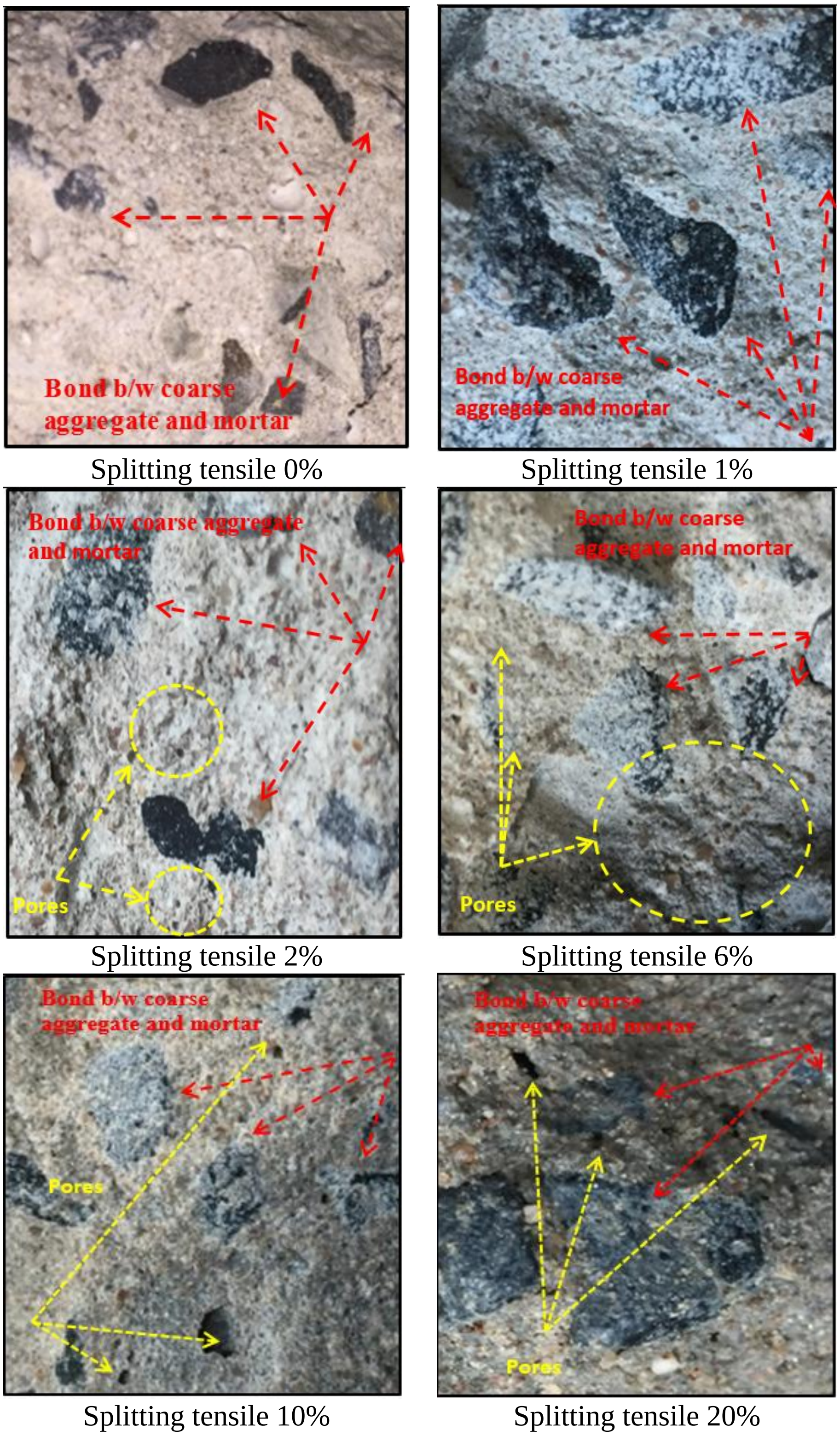

Figure 16 Fracture surface of the concrete with oil contaminated sand

Figure 17: Failure modes of different samples due to pull out test

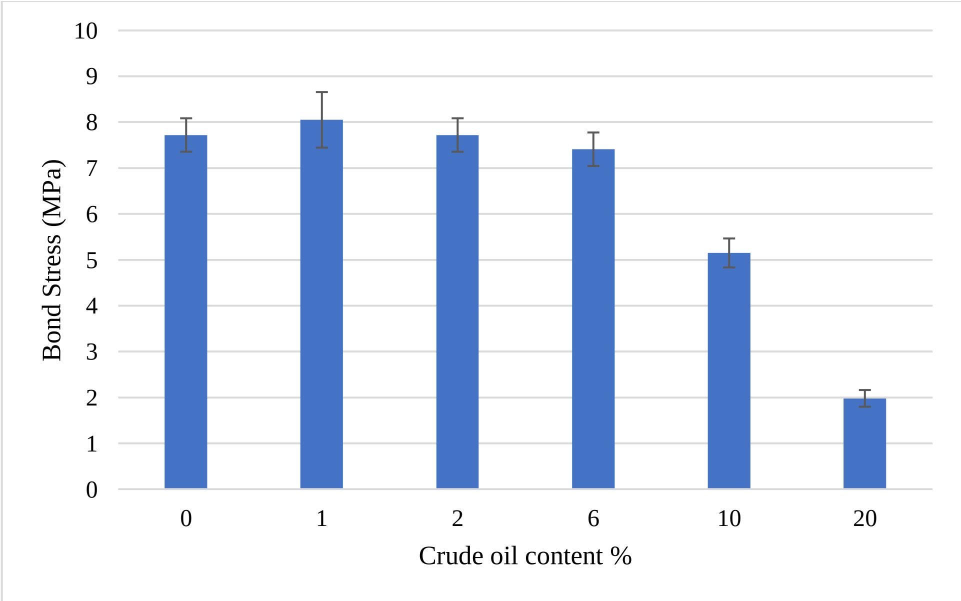

Figure 18: Bond strength of pull-out bar with different percentages of crude oil

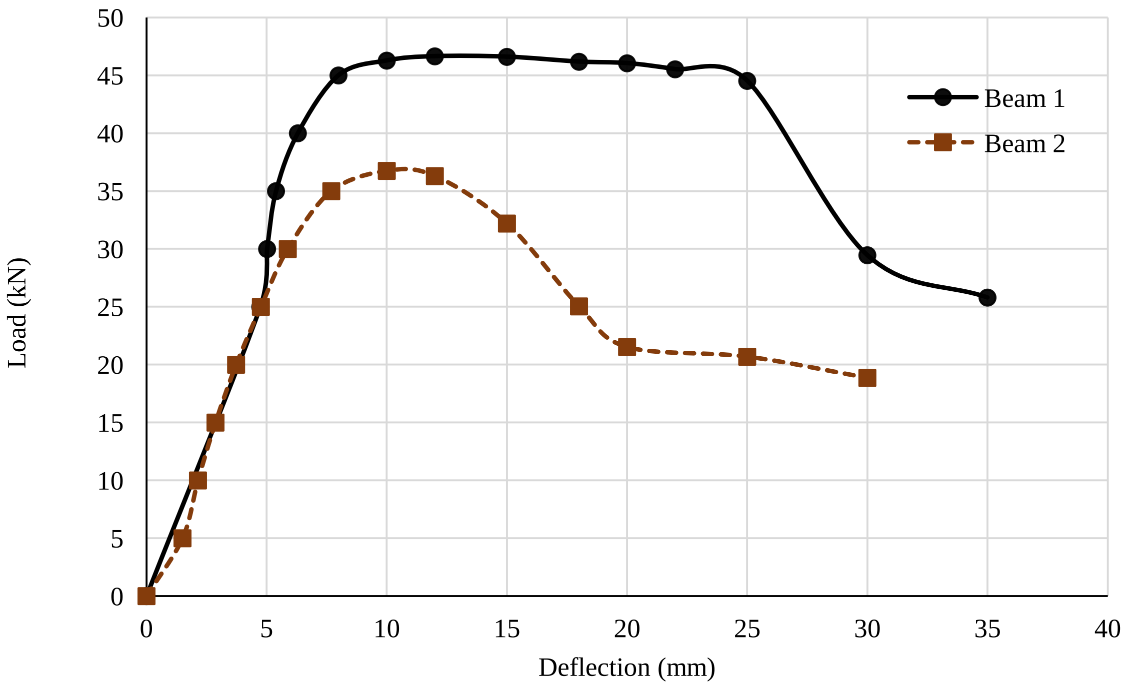

Figure19: Load-Displacement behaviour and failure behaviour of beam 1 without oil and beam 2 with oil contamination

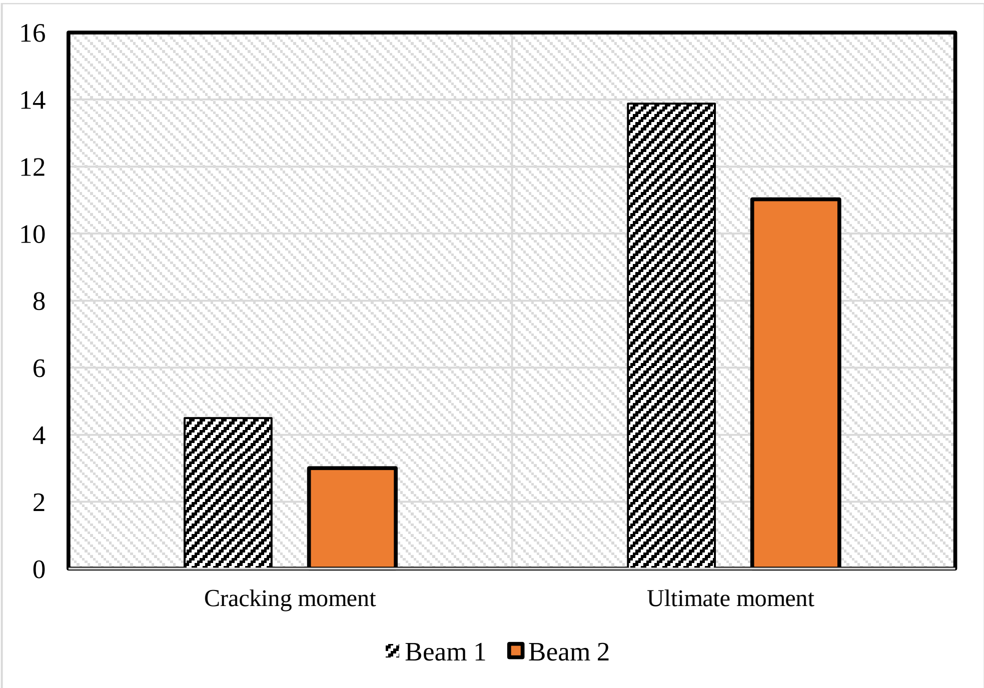

Figure 20 shows the comparison of the cracking and ultimate moment of beam 1 and beam 2.

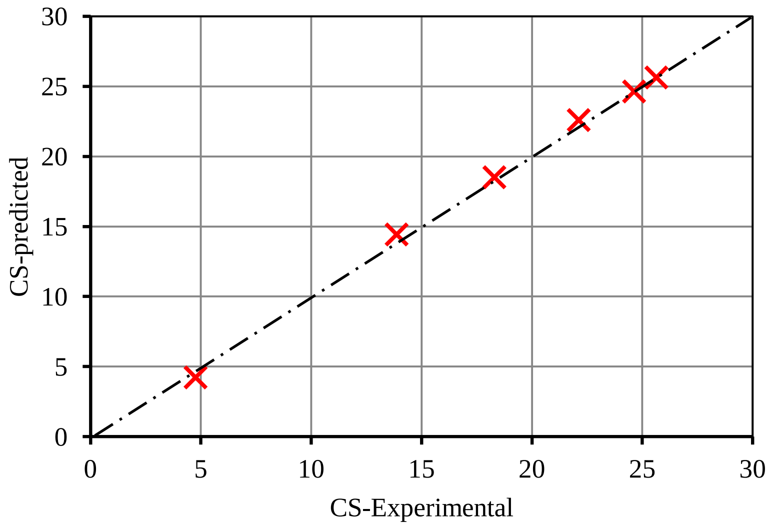

Figure 21 Validation of the proposed equation of the compressive strength of concrete containing crude oil with simulation results

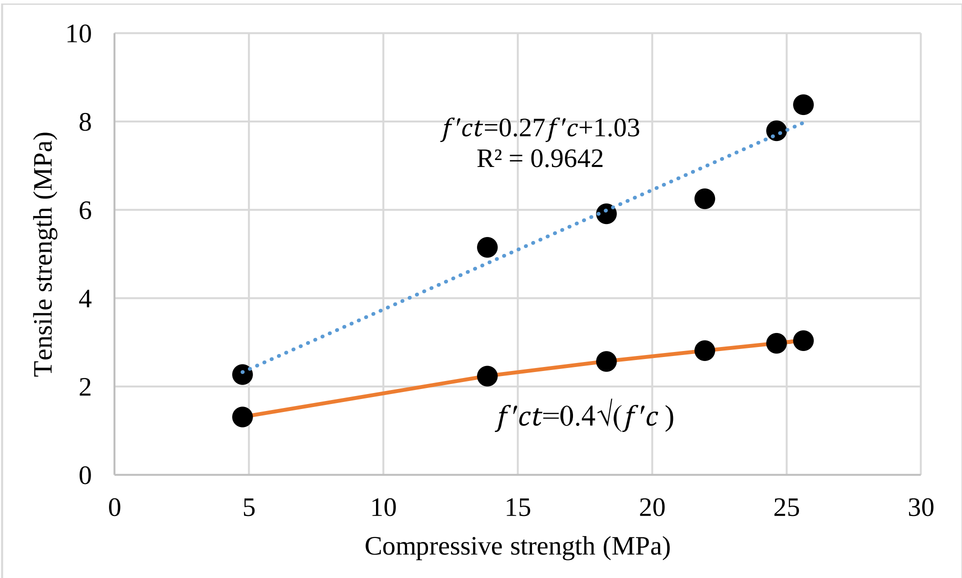

(5)

Figure 22: Tensile and compressive strength relationship

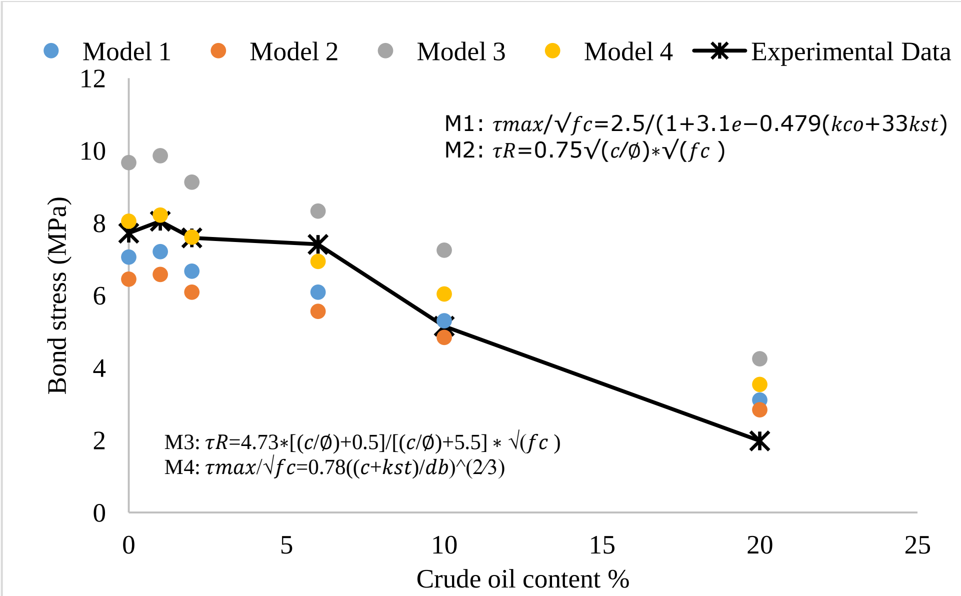

Figure 23: shows the bond strength models plotted against percentage contamination level.

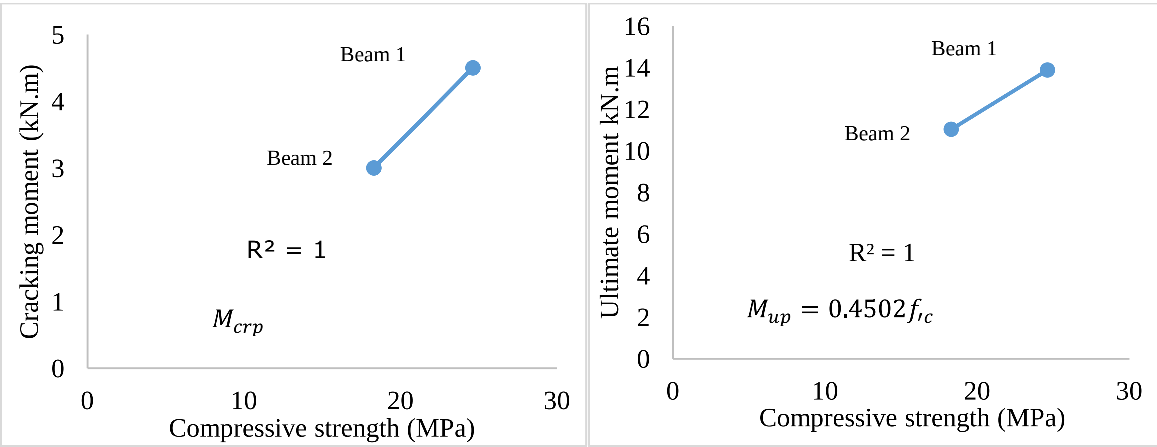

Figure 24: Developed equations of cracking and ultimate moment of uncontaminated beam (beam 1) and contaminated beam (beam 2).

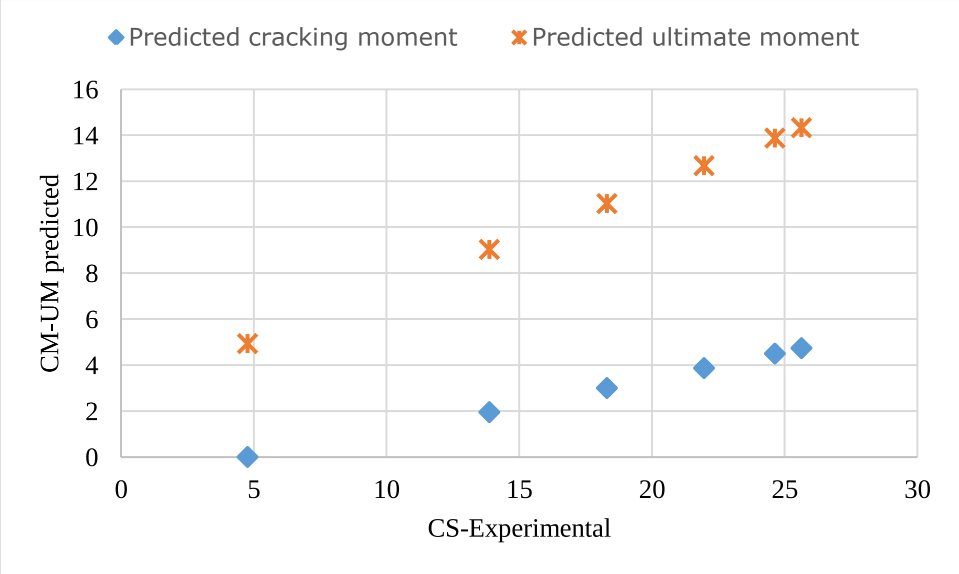

Figure 25: Shows the results of the proposed equation of the cracking and ultimate moment of concrete containing crude oil

*Highlights

Journal title: Construction and Building Materials

Title: Properties and structural behavior of concrete containing fine sand contaminated with light crude oil

Authors: Rajab Abousninaab*, Allan Manaloa, Weena Lokugea, and Khalifa Saif Al-Jabrib

Highlights of the paper

- The physical, mechanical, and microstructure of concrete containing fine sand with different levels of light crude oil contamination (0, 1, 2, 6, 10 and 20%) were investigated
- The effect of light crude oil on the bond strength and flexural strength of reinforced concrete was conducted
- Simplified empirical equations were also proposed to reliably predict the mechanical properties of concrete containing oil contaminated sand

Properties and structural behavior of concrete containing fine sand contaminated with light crude oil

Rajab M. Abousnina*, Allan Manalo, Weena Lokuge, Khalifa Saif Al-Jabri

Graphical Abstract

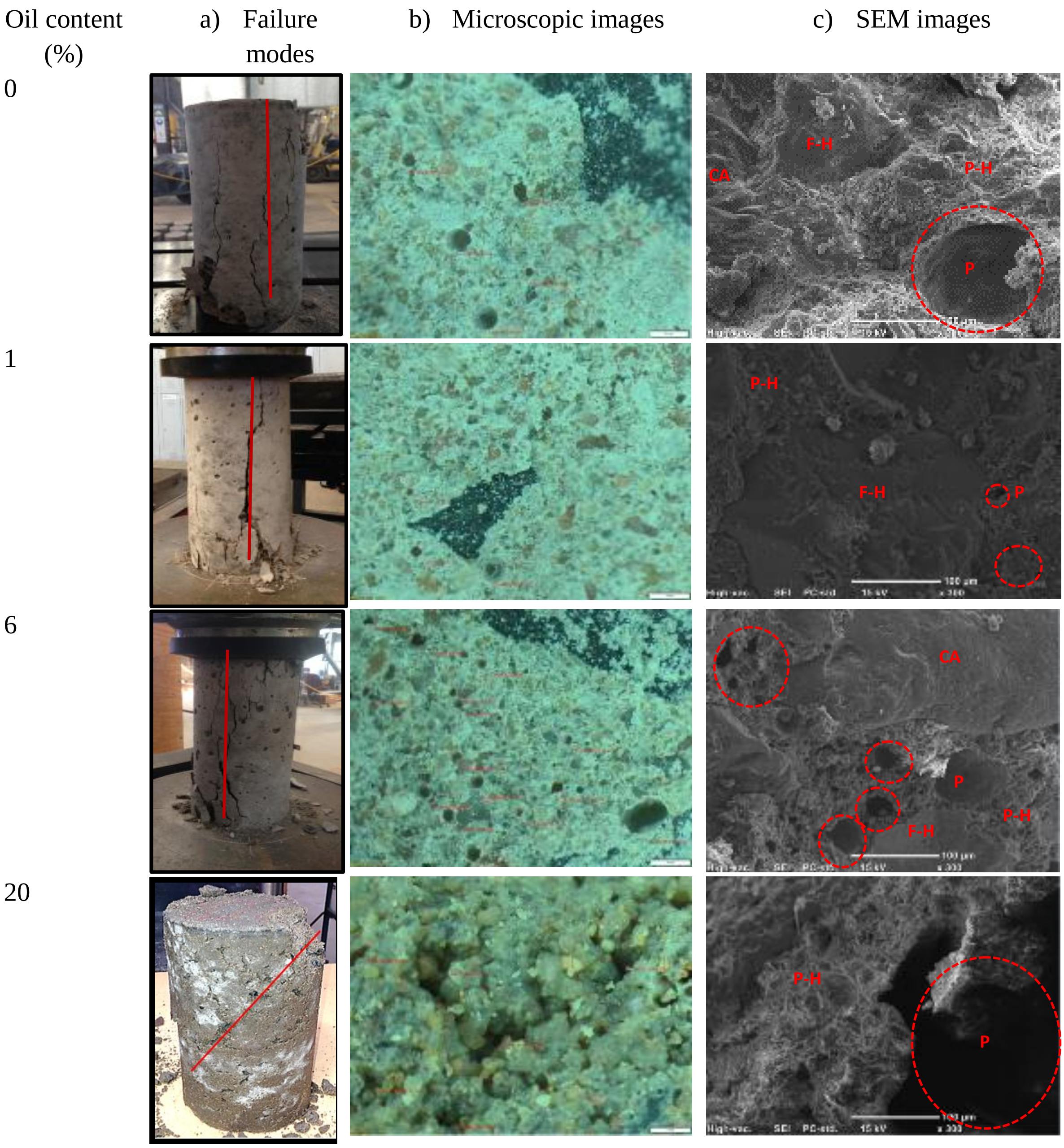

Properties of concrete containing fine sand with tipical light oil contamination (0, 1, 6 and 20%)

Properties and structural behavior of concrete containing fine sand contaminated with light crude oil

Rajab Abousnina[ab*], Allan Manalo[a], Weena Lokuge[a], and Khalifa Saif Al-Jabri[b]

[a] Centre for Future Materials, School of Civil Engineering and Surveying,
University of Southern Queensland, Toowoomba, Queensland 4350, Australia
Tel. +61 7 46311331.

[b] Department of Civil and Architectural Engineering, PO Box 33, College of Engineering,
Sultan Qaboos University, Al-Khod 123, Oman Tel. +968 2414 1332

Abstract

Mixing crude oil contaminated sand with cement and using this mix as an alternative construction material is considered an innovative and cost-effective approach to reduce its negative environmental impact. In this study, the compressive and splitting tensile strength of concrete with different levels of light crude oil contamination (0, 1, 2, 6, 10 and 20%) were evaluated. Microstructure observation was also conducted to better understand how the oil contamination is affecting the concrete properties. The bond strength of steel reinforcement and a comparative evaluation of the flexural behaviour of steel reinforced beams using concrete with 0% and 6% oil contamination was carried out. Results showed that concrete with light crude oil contamination can retain most of its compressive and splitting tensile strength at a contamination level of up to 6%. A good bond between the steel reinforcement and concrete can be achieved up to this level of oil contamination. The concrete beam with 6% oil contamination exhibited only a 20% reduction in the moment capacity compared to a

beam using uncontaminated concrete. Simplified empirical equations were also proposed to reliably predict the mechanical properties of concrete containing oil contaminated sand.

Keywords: concrete; oil contamination; mechanical properties; bond strength; bending.

1. Introduction

There is a growing public concern about the adverse environmental effect caused by the petroleum hydrocarbons that are generated from oil leakage or spill [1]. In the last two decades, there has been significant number of oil spills around the world in tens of thousands of litres and the general trend appears to be continuing, despite the stricter environmental regulations, be either on land or at sea. For instance, it was reported that about 1.1 billion litres of crude oil in Kuwait was purposely spilt into the Arabian Gulf, the Persian Gulf, and in Kuwait desert between August 1990 and February 1991 [2]. These are considered to be the largest oil spills in history [2, 3]. As a consequence of this intentional leakage, 700 km of coastlines were severely polluted between Kuwait and Saudi Arabia, and approximately 49 square kilometres of the Kuwait desert was affected. Furthermore, the explosion of the British petroleum BP deep water horizon drilling rig in the Gulf of Mexico in 2010 caused a spill of around 91 million litres of oil that has affected about 110 km of the Louisiana coastline [4, 5]. Moreover, in 2009 an incident of oil spillage caused by Pacific Adventurer in Moreton Bay contaminated various Queensland Beaches [6]. The clean-up of these shorelines and land areas is a challenging and expensive task depending on the level of the oil spill, for example, the clean-up after the oil spill from Pacific Adventurer cost over $34 million and involved 2500 people [6]. The oil spill contamination impacts on the properties of the surrounding sand and changes its physical and chemical properties [7]. In order to minimise its effect on the environment, remediation methods ranging from sand washing, bio-remediation, electro-kinetic sand remediation, and thermal desorption have been implemented, but are not considered to be cost effective [8]. Thus, a number of researchers

[9-11] suggested that an alternative and effective method of remediation is using contaminated sand in engineering applications. Their results showed that the properties of concrete were affected by crude oil, however, the severity of this effectiveness was based on the amount of oil in concrete. Based on that, they have concluded that sand contaminated with oil can be used in some engineering applications.

It is well known that the successful use of waste materials in concrete depends on the developed mechanical properties of the end product. While some studies investigated the effects of oil contamination on concrete, these studies have focussed only on heavy crude oil and engine oil [12-14] as well as hydrocarbons [14-16]. For instance, Almabrok, et al. [17] investigated the effect of mineral oil on the cement solidification process, and its consequent effect on the fresh and hardened properties of mortar. Almabrok, et al. [18] further investigated oil solidification using a direct immobilization method. Similarly, the effect of kerosene contaminated sand on the compressive strength of concrete in different exposure conditions was investigated by H. Shahrabadi and D. Vafaei [19]. Their results showed that using contaminated sand adversely affected the compressive strength of concrete (a reduction up to 27% in the concrete compressive strength was occurred in 2% kerosene contaminated samples). Attom M., et al. [20] investigated the effect of kerosene and diesel at different percentages (0.5, 1 and 1.5% by dry weight of sand) on the compressive strength of concrete and a noticeable reduction up to 42% was observed. Recently, Shafiq, et al. [21] have investigated the effects of engine oil (UEO) on slump, compressive strength and oxygen permeability of normal and blended cement concrete. They concluded that the engine oil in concrete caused a reasonable reduction in the total porosity, and the coefficient of oxygen permeability of all concrete mixes as compared to uncontaminated concrete. A recent study conducted by Abousnina, et al. [22], investigated the effects of light crude oil contamination on the physical and mechanical properties of geopolymer cement mortars. The results showed that geopolymer mortar has the potential of utilizing oil contaminated sand, and reducing its environmental impacts.

Light crude oils and refined products tend to be more toxic than those of heavy crude oils as heavy crude oils have a higher average molecular weight. The hydrocarbon families are the low-boiling-point aromatics, particularly benzene, toluene and xylene. The most toxic hydrocarbons also tend to have a high solubility in water. A high solubility makes a molecule more accessible for uptake by plants and animals. The toxicity of a given hydrocarbon varies considerably with the organism exposed [23]. Moreover, most studies have focused only on the characterisation of the mechanical properties of the produced concrete and none have investigated the behaviour of concrete structures utilising this waste material.

This study presents an extensive investigation that was conducted to evaluate the effects of light crude oil on the mechanical properties and microstructure of concrete. In addition, a comparative study of the bond strength and flexural strength of reinforced concrete containing oil contaminated sand was conducted. Data analysis and modelling was also implemented to develop simplified equations to describe the mechanical properties of a concrete mix containing fine sand contaminated with light crude oil. The outcome of this study will provide useful information on the use of oil contaminated sand in building and construction which will be cost-effective alternative remediation method for the waste material.

2. Materials and methods

2.1 Materials

2.1.1 Fine aggregate

The fine sand was air dried and the Particle Size Distribution (PSD) shown in Figure 1 was determined following the AS 1141.11.1-2009 [24]. The particle grading curve of fine sand showed that the grain size of the sand particle is less than 2.36 mm.

Figure 1: Particle size distribution curve of the sand

2.1.2 Coarse aggregate

The coarse aggregates had a maximum size of 10 mm and the particle size distribution of coarse aggregates is presented in Table 1. The coarse aggregates used were in Saturated Surface Dry (SSD) condition.

Table 1: Sieve analysis of coarse aggregates

2.1.3 Cement and water

Ordinary Portland cement [25] and clean potable water were used in the concrete mix.

2.1.4 Light Crude Oil

Mineral Fork w2.5 motor cycle oil was used as light crude oil. This oil was selected because its density and viscosity are very similar to light crude oil as shown in Table 2.

Table 2: Comparison between light crude oil and Fork w2.5 Motorcycle oil [26, 27]

2.2 Specimens details

Table 3 shows the types of tests and specimen details to study the effect of oil contaminated sand (up to 20%) on the compressive strength, tensile strength and bond slip of concrete. A total of 18 samples (100 mm diameter and 200 mm high cylinders) were cast for each test.

The most ideal crude oil contamination of 6% was selected for beams and compared with the uncontaminated beam (0%). All specimens were tested after 28 days of curing.

Table 3: Tests conducted and specimen details

2.3 Specimen preparation

2.3.1 Preparation of oil contaminated sand

The contaminated samples were prepared by mixing the dry sand with different percentages of light crude oil (1%, 2%, 6%, 10%, and 20%) according to the weight of the dry sand. These percentages were considered based on the results obtained from previous studies [28, 29]. In addition, the uncontaminated (0%) sand was used in the control sample (Figure 2). A maximum of 20% contamination was selected because the contaminated sand was already saturated and any additional oil would just drain from the sand. This would make some tests, for example for shear strength and permeability, difficult to conduct and may lead to less reliable results [30]. The oil was mixed manually with dry sand and then the samples were placed inside a plastic container for 72 hours to allow the mixture to attain a homogenous condition. A lid was placed on the plastic container to prevent the crude oil from evaporating during the period of incubation.

Figure 2: Contaminated sand with different percentages of oil (0%-20%)

2.3.2 Mixing and preparing concrete cylinders

Concrete was prepared based on AS 1012.2 [31], with mix proportions of 1 part of cement to 3 parts of fine sand and 3 parts of coarse aggregate (10 mm), and with water-to-cement ratio (w/c) of 0.5. Mixing was performed using a 120L Portable Electric Concrete Mixer. Plastic moulds (100 mm diameter and 200 mm high) were used to avoid any contamination and for easy removal of the cylindrical specimens. Concrete was prepared at a room temperature of around 22ºC ± 2, while the curing took place in a fog room with 25 ºC and 85% humidity for 28 days.

2.3.3 Specimens for bond strength

The bond-slip specimens were prepared such that the bars were positioned concentrically (before casting of concrete) within the horizontally cast 150 mm x 150 mm x 300 mm concrete prisms with different crude oil content (0, 1, 2, 6, 10 and 20%) as shown Figure 3. The reinforcing bars used were 16 mm-diameter deformed steel bars with a yield strength of 500 MPa and a nominal length of 700 mm. The steel bars were free from any rust or other contaminants. The bond slip testing specimens were 18 in total, 3 specimens for each level of oil contamination.

Figure 3: Bond-slip specimens

2.3.4 Beam specimens

Two beams each of length 1400 mm, 250 mm depth and 100 mm width were used. Beam 1 is the control beam with no oil contamination and beam 2 is contaminated with 6% light crude oil. The beams were reinforced with 2N10 bars at top and bottom, and 6 mm diameter stirrups spaced at 100 mm centre to centre. Concrete spacers of 25 mm were used in between reinforcement and the mould for the concrete cover as shown in Figure 4.

Figure 4: Beam reinforcement details

Concrete was mixed in a concrete mixer and placed into steel moulds. While casting, the concrete was vibrated using an electrical vibrator. After the casting process, the beams were cured for 28 days before testing.

2.4 Test set-up and procedure

2.4.1 Void measurement and microscopic observations

Typical normal strength Portland cement concrete usually has a density of approximately 2400 kg/m^3 and varies depending on the amount and the density of aggregate, air voids, water-to-cement ratio, and the maximum size of aggregate used [32]. Thus, prior to conducting the mechanical tests, the density of the test specimens was estimated through the measured mass and volume of each specimen. Moreover, visual observation of the pore sizes and distribution was conducted for all specimens. A microscope (Motic SMZ-168 series) was used, to examine the microstructure and to measure the pore diameters at the fracture surface of the tested concrete cylinders. The results were compared with the microstructure observed using a scanning electron microscope (SEM) (JEOL JCM-6000, Tokyo, Japan),

2.4.2 Compressive and splitting tensile strength tests

Compressive strength test of concrete cylinders with different levels of crude oil contamination was conducted following the procedures prescribed in AS-1012.9 [33]. The specimens were tested to failure using a 2000 kN SANS hydraulic compression and tensile testing machine). The load was applied at a rate of 2 mm/min. The maximum load applied to the specimen was then recorded and the type of failure was noted. An average of three samples was taken as representative of the compressive strength of the concrete cylinders.

Splitting tensile test was conducted as per AS-1012.10 [34]. The test was carried out by placing a cylindrical specimen horizontally between the load surfaces of a 2000 kN capacity servo hydraulic testing machine a rate of 2 mm/min until failure of the cylinder was observed. An average of three samples was taken as representative of the splitting tensile strength of the concrete cylinders.

2.4.3 Bond strength test

Figure 5 shows a schematic diagram and the actual set-up of direct pull-out test employed in this study. The test was conducted in accordance with (ACI) [35]. The specimens were positioned upside down while the bars were being pulled downward at a constant rate of 1.2 mm/min using an AVERY testing machine. A single Linear Variable Differential Transducer (LVDT) was placed at the end of the steel to measure the overall slip relative to concrete. The support stand of LVDT was placed separately from the test specimen to ensure that the movements of the specimens during the loading stage or the failure of the specimens does not affect the measurements. The pull-out load and end-slip were measured and recorded using System 5000 data logger.

Figure 5: Direct pull-out test in accordance with ACI 440.3R-04

2.4.4 Flexural strength test of beams

The test is conducted in 2000 kN SANS apparatus which consists of a base, upper platen which is attached to the upper crosshead as shown in Figure 6. The lower platen is attached to a hydraulic mechanism to adjust its height. The sample is placed between upper and lower platen. Data were recorded using the computer software designed for SANS.

Figure 6: SANS testing machine

3-point static bending test was used to evaluate the flexural behaviour of the beams. Grid lines were drawn on the beams for the easier observation of crack development and beam deformation. The specimen was placed at the loading base as shown above in Figure 6. The upper and lower platens were adjusted in such a way that the load is applied at the centre of the beam. The loads were applied in a uniform pattern, any cracks or deformation formed were marked on the beam.

3. Discussion of the Experimental Results

3.1 Physical, mechanical and microstructure properties of concrete with oil contaminated sand

3.1.1 Surface voids and density

A number of visual differences was observed for the specimens containing different percentage of light crude oil contaminations. For instance, increasing the crude oil content increases the surface voids as well as the wetness of the specimens, as shown in Figure 7. The surface voids were clearly observed with 6% of light crude oil contaminations and they became larger in size and more distributed over the surface for 10% and 20%. Similarly, the wetness was more noticeable for specimens with 10% and 20% of light crude oil contamination than for the other specimens. In these specimens, dark patches of oil could be clearly seen on the surface. Moreover, the specimens with 20% crude oil contamination were excessively saturated with oil appearing to be dark brown in colour, and the oil smell was strong.

Figure 7: Surface voids of concrete with different levels of crude oil contamination

Figure 8 shows the total bulk density of the concrete with different crude oil contaminations. It can be observed that the crude oil content affects the density of the concrete. As crude oil content increases, the density of the specimens decreases. The highest average density was

2439.5 kg/m^3 (for uncontaminated samples) whereas the lowest density was 2240.7 kg/m^3 for specimens with 20% crude oil contamination. This can be explained by the surface voids observed in the specimens, which progressively became apparent as the oil contamination is increased, resulting in a decrease in the density.

Figure 8: Density of specimens with different levels of oil contamination

Increasing the crude oil content affected both the concrete porosity and the wetness of the specimens. After 28 days of curing, samples with 20% oil contamination were seen excessively porous and saturated, as shown in Figure 7. Increase in the porosity at high levels of oil contamination was due to the water seepage during curing. As evidence, water was found in the plastic bags that were used to cover the specimens during curing, especially for specimens with an oil contamination above 6%. Almabrok, et al. [36] also suspected that the water absorption during curing was prevented due to the saturation status caused by crude oil contamination. A study by Madderom and President [37] demonstrated that extra water increased the concrete porosity and hence, the pores act as reservoirs that were formed around the aggregates. As a result of over-saturation, air pockets were formed. They further indicated that cement and fine particles carried outwards during seepage weaken the concrete surface by around 20%. Thus, the pores appearing on the surface of the specimens could be due to the vertical water channels and oil seeping from the concrete surface. As a result of porosity, density of the hardened concrete decreased as the amount of crude oil increased.

3.2 Effects of oil contamination on the strength of concrete

3.2.1 Failure mode of the specimens

The failure mechanisms of the samples provide an indication of the variation of the compressive strength of the specimens. Most specimens with 0% to 6% oil contamination displayed a splitting-type failure, as shown in Figure 9. This failure mode (splitting failure) occurred from the bottom cap and travelled perpendicular to the load. On the other hand, increasing the level of light crude oil contamination to 10% and 20% resulted in the specimens failing in shear, with crushing at the top. The crushing occurred due to the saturation status of the concrete cylinders with light crude oil contaminations leading to a lower compressive strength.

Figure 9: Failure modes of specimens containing different crude oil content. (splitting shear failures with and without fracture)

3.2.2 Compressive strength of concrete

Figure 10 shows the average compressive strength of the concrete with different levels of oil contamination. It can be clearly seen that the increase in the level of light crude oil contamination results in a decrease in the concrete compressive strength. Nevertheless, the compressive strength of concrete with 1% light crude oil contamination is 3.2% higher than the uncontaminated samples. The compressive strength decreased considerably at 10% and 20% light crude oil contamination.

The increase in strength may be attributed to oil optimising concrete cohesion, without causing water seepage. Abousnina, et al. [30] found that sand contaminated with 1% of light crude oil achieved an optimum sand cohesion of 10.76 kPa. As a consequence, the total porosity and the average of pore diameter at 1% was less than that at 0%, as shown in Figure 12. Above 1%, sand became saturated with oil, resulting in a reduced compressive strength. This reduction in compressive strength may be due to incompletion of the hydration process at 28 days of curing for concrete with high level of crude oil contents. Furthermore, increasing the light crude oil from 2% to 20% may have hindered the formation of strong bond between the paste and aggregate particles, as the oil was coating sand and coarse aggregate particles. As shown in Figure 11, excess oil was present in the space previously occupied by aggregates. When the aggregates exceed the saturated surface dry condition (SSD), a damp or wet status is achieved where all the pores are completely filled with oil [38]. Thus, the surface area that is able to bond with cement mortar is decreased, leaving the aggregates surrounded by a barrier of oil. Similarly, the formation of oil around sand particles acts as a cushion preventing inter-particle contact, and the lack of cohesion promotes slippage between the sand particles. After seepage of water, air voids are left and the result is a relatively porous cement paste that has a low internal strength, hence limiting the ultimate compressive strength of concrete.

Figure 10: Average compressive strength of specimens with different crude oil content

Figure 11: Moisture conditions of aggregate (sand, coarse) compared to that observed at a high level of crude oil content (10% and 20%)

However, the reduction in the compressive strength of concrete containing contaminated fine sand at a high level of light crude oil (i.e. beyond 6%) can be further explained by the increase in the pore sizes. Figure 12 shows that with the increase of the crude oil content from 2% to 20%, the number and the size of pores increase. This is due to the free water in the concrete mix that was not utilised during the hydration process, creating pores in the concrete paste. These pores transcend even at the surface of the specimens, as shown in Figure 7.

Figure 12: Pore size diameter of concrete with light crude oil contamination

3.2.3 Relationship between porosity, microstructure and compressive strength

The porosity of the specimens with different crude oil content obtained by visual observation, microscopic images and SEM, is shown in Figure 13. Based on the visual observation, the pore size and the pore distribution were found to decreases lightly for concrete with 1% of light crude oil contamination, compared to uncontaminated samples (0%). This was attributed to the sand reaching optimum cohesion as a result of oil binding sand particles, confirmed by previous investigation [39]. Thus, higher strength of concrete with this level of oil contamination was obtained compared to uncontaminated concrete. In contrast, increasing the crude oil contamination level from 2% up to 20% increases both the sizes and distributions of the pores. From the microscopic observations, the average pore size in the uncontaminated samples was 454 μm, but it is only 368 μm for 1% of crude oil contamination. This increased to 446 μm, 500 μm, 720 μm, and 877 μm for 2%, 6%, 10%, and 20% oil of contamination, respectively. Furthermore, the interconnection between the large pores, as well as the wettability of the specimens, was high at 20% of crude oil contaminations.

The SEM images presented in Figure 13 can be divided into full hydrated cement (F-H), partially hydrated cement (P-H), pores (P), and the coarse aggregate (CA). In these images, it can be noticed that the pore sizes and P-H area were smaller for 1% of crude oil contamination than for uncontaminated samples, which is an indication of an enhancement in hydration process at this percentage. However, as the amount of crude oil increases above 1%, the F-H decreased, while the P-H and pore size increased.

Figure 13: Porosity of the specimens with different crude oil content through visual observation, microscopic images and SEM

From the three observation methods used (visual observation, microscopic and SEM), it can be seen that the size and distribution of the pores increased as the amount of crude oil increased (from 2% to 20%). As oil is hydrophobic, the molecules of oil will bond much more readily with each other than with the water molecules, creating a barrier to the surface of aggregate particles. As a result, this decreases the contact between the cement paste and the aggregates. Moreover, some of the water added to the concrete mix will remain free, creating more and bigger pores compared to uncontaminated samples. Kim, et al. [40] stated that any excess water can cause segregation of the aggregates and degradation of strength and durability. In this study the authors have further indicated that in a normal concrete mix with the same cement content, hydration can be more easily activated with larger unit of water content. Despite this, the excess water used for hydration reaction in the cement paste created more pores, which led to a reduction in compressive strength, even with the same amount of hydration products.

3.3.3 Splitting tensile strength of concrete with oil contaminated sand

3.3.3.1 Failure modes

Figure 14 shows typical splitting tensile failure modes of the concrete specimens with different crude oil contaminations. Furthermore, the distribution of the coarse aggregates can be clearly seen at the high level of crude oil contamination. This may be due to large percentage of crude oil which increased the workability and hence, it partly segregated and caused discontinued distribution of solid materials. An initial indication of failure under the splitting tensile test was the audible cracking noises that were heard during testing. The noise was clearly heard for up to 6% of crude oil contamination but it decreased for 10% and 20%. Observation inside the specimens clearly showed that the crude oil filling the voids of cylinders with 10% and 20% contaminations but could hardly be noticed in 1% to 4%. The oil appeared in the form of crystallised yellow particles, (crude oil 6%).

Figure 14: Splitting tensile failure modes of concrete with different crude oil content

3.3.2 Tensile strength of concrete

Figure 15 shows the relationship between the splitting tensile strength of concrete at 28 days of curing, and the levels of crude oil contamination. The specimens with 1% of crude oil contamination showed a 6.9% higher splitting tensile strength, compared to uncontaminated samples (0%). In contrast, increasing the crude oil contamination to 2%, 6% and 10% decreased the tensile strength by 19%, 24%, and 33%, respectively; while at 20% of light crude oil contamination, a reduction of 70% was observed. These results indicate that the splitting tensile strength of concrete was enhanced by adding light crude oil content up to 1% but beyond this, the tensile strength decreased. The increase in strength was attributed to the sand reaching optimum cohesion at this level of oil contamination, as a result of oil binding sand particles. On the other hand, increasing the crude oil content above 2% caused the fine sand to exceed the equilibrium condition, and the oil also contaminated the surface of the coarse aggregates. As a consequence, the bond between the cement paste and coarse aggregates was affected, resulting in a decrease in tensile strength. Figure 16 shows that the failure of the specimens occurred between the cement paste and the surfaces of the largest coarse aggregate particles which indicates a bond failure mode.

Figure 15: Splitting tensile strength test results of oil contaminated concrete

At 6% to 20% oil contamination level, the aggregate particles were expected to be fully covered by oil. This oil creates a thick film over the surface of the aggregates, which decrease their bond with the cement paste, as oil is a hydrophobic material. However, it was observed that emulsion was created at the surface of the aggregates. The soft particles of fine sand and cement particles can act as the emulsifying agent because they can work as finely dispersed solids.

Figure 16 shows cement particles attached to the surface area of the coarse aggregates with up to 10% in crude oil contaminations. However, at 20% of crude oil contaminations, the cement particles could not be seen at the surface area of the coarse aggregates, due to high saturation status of the concrete mix by the crude oil at 20%. As a result, the interaction between the oil/water and the fine particles was far from the surface of the aggregates. Thus, the crude oil worked as an isolator, preventing development of strong bond between the cement paste and the aggregates, and thus resulting in lower tensile strength.

Figure 16: Fracture surface of the concrete with oil contaminated sand

3.4. Pull-out behaviour of steel in concrete with oil contamination

3.4.1 Failure modes

Two types of failure modes were observed with different oil contamination: yielding of the pull-out bar and splitting failure of the rectangular concrete prism as shown in Figure 17. Samples with oil-contaminated sand of 0, 1, 2 and two samples of 6% of oil contaminated sand were failed due to yielding of the bars. However, the third sample of 6% as well as 10 and 20% of crude oil contamination were failed by splitting of the rectangular concrete prisms. The failure of the third sample with 6% contaminated oil was accompanied by a loud explosive noise indicating the brittle nature of failure. In this sample, it was observed that the sample had radial cracks which propagated from the steel bar to the top surface hence splitting the sample. Then it was further split open and the steel bar was stuck to one half of the sample and it came off after a gentle knock. There were small voids that could be seen on the broken surface of the sample. The pull-out bar appeared to have concrete stuck between the ribs of the bar.

Figure 17: Failure modes of different samples due to pull out test

In case of specimens with 10% of crude oil contaminations all samples failed under splitting failure as clearly seen in Figure 17. The sample failed with a loud explosive noise but the noise level was lower than the 6% second sample. Cracks appeared to propagate radially on the concrete prism from the steel bar towards the surface, similar to the 6% sample. Void spaces were also noticed on the broken surface of the samples. The pull-out bar was observed to have less concrete between the ribs of the bar. Similarly, with 20% of crude oil contamination both samples failed under splitting failure as shown in Figure 17. It failed with a loud noise but the noise level was lower than the previous samples. Cracks appeared to propagate radially on the concrete prism from the steel bar towards the surface. Close examination of the broken samples revealed void spaces on the broken surface of the samples. The embedded section of the pull-out steel bar was noted to have minimal concrete residue between the steel ribs. It also appeared damp with oil residue and shiny surface. The pull-out steel bar of the third 6% sample was also observed to have concrete between its steel ribs. The 10% sample was observed to have lesser amount of concrete between ribs than the 6% sample and, 20% sample appeared to have even lesser amount of crushed concrete between ribs as shown in Figure 17.

Literature review indicates that chemical adhesions and frictional resistance are the first two mechanisms to break at low loads. However, mechanical interlock, created by the ribs of the deformed bar, is the key mechanism that contributes to bond strength. The failure mode produced due to mechanical interlock are generally splitting failure and, pull-out failure for very weak concrete. Splitting failure occurs when the concrete is crushed in front of the steel ribs lifting the concrete key, hence inducing a hoop stress within. Crushed concrete in front of ribs were visible for 6% (sample 3) and the amount of crushed concrete decreased for 10% contamination level and there was very less amount of crushed concrete visible for 20% samples. This indicates a gradual loss of bond in 10% and 20% samples compared to the 6% samples.

4.2 Failure load of specimens from pull-out tests

Failure load, bond stress, change in length of pull-out bar with different percentages of crude oil are presented in Figure 18. It can be seen that the samples with up to 6% of crude oil contaminations failed under the yielding of the pull-out steel bars, that is, the steel bar yielded while the concrete prism remained intact. For samples with 10% and 20% contamination levels, the average bond strengths are 33.25% and 74.36% lower than the control sample, respectively. These were observed to have radial cracks on the concrete prism which developed at the steel bar and continued to the surface of the concrete prism. However, none of the specimen failed under direct pull out failure.

The significantly lower bond strength of 20% oil contaminated samples and more than one third loss of strength of 10% samples can again be attributed to the state of wetness of the sand particles as described by [30], Abousnina, et al. [41]. Their microscopic study of sand particles showed that the 20% oil contaminated samples are in a saturated state where the surface area of the sand particles was fully coated with oil, hence, it formed a barrier for the water and cement to fully come in contact with the sand particles. This hindered the development of bond, firstly, between the individual sand and coarse aggregate particles and secondly, between concrete and steel.

Figure 18: Bond strength of pull-out bar with different percentages of crude oil

3.5. Comparative evaluation of concrete beams with and without oil contamination

As shown in Figure 19, the load was applied at the mid-span of the beam in a uniform rate. Cracks started in the uncontaminated beam at the bottom near the centre portion at about 15 kN load level. The load-displacement behaviour of the uncontaminated beam (control) is shown in Figure 19 (beam 1). The first crack formed in beam 1 (uncontaminated beam) at 15 kN load , and before reaching the first crack the stiffness of the beam remained steady, however, after the cracking the stiffness decreased. As the load increased, the crack and the deflection increased for instance, when the load reached 25 kN, the deflection was 4.7 mm which then progressed in a steady state till 35 kN showing a deflection of 5.4 mm. When the load reached 46.3 kN, the beam started yielding and progressed to a deflection of 25 mm with load reaching 44.53 kN and then beam started failing and at 25.8 kN the beam completely failed showing a deflection of 35 mm. The beam after yielding at 46.28 kN, the deflection progressed in a steady state till 44.53 kN which indicates the strong bonding between the concrete and the steel.

Figure 19: Load-displacement behaviour and failure pattern of beam 1 without oil and beam 2 with oil contamination

On the other hand, the cracks in the oil contaminated beam (beam 2) were formed in a similar pattern as that of beam 1. The first crack formed in beam 2 was at 10 kN with a deflection of 2.9 mm. However, as the load increased, the number of cracks and the deflection increased. Hence, when the load reached 25kN it showed a deflection of 4.8mm which then progressed, at load level of 35kN, a deflection of 7.7mm was reached. At 36.8kN, the beam started yielding showing a deflection of 10mm and progressed to a deflection of 12mm with load reaching 36.3KN and then beam started failing. At 18.9 kN the beam completely failed showing a deflection of 30mm. Unlike beam 1, beam 2 showed a sudden failure after yielding at 36.8kN,. The maximum load for beam1 was 20.5% higher than that of the beam 2 (with 6% of crude oil contamination). Furthermore, the initial stiffness of both the beams were similar. The change in stiffness occurred after the formation of cracks on both beams. The stiffness directly depends on the ultimate load, more the ultimate load more will be the stiffness. In beam 2, the presence of oil has resulted in the diversion of stiffness. The presence of oil affects the adhesive property of the concrete resulting in the slip. This behaviour agrees with a previous study conducted by Abednego et al. [42], on the effect of crude oil contaminant in the engineering properties of concrete. They concluded that the presence of crude oil delays the process in the gel and it also weakens the cohesiveness of the binder’s paste.

As mentioned earlier that the first crack was formed at 15kN for beam 1, while the initial cracking of the second beam (with 6% of crude oil contamination, beam 2) was observed at 10kN. It can be seen that the cracking moment of the beam 1 (uncontaminated beam) is higher by 33% compared to beam 2 (with 6% of crude oil contamination). This agrees with the initial observation of the cracking as the initial crack of beam 1 was observed at 15kN while the cracks of beam 2 was observed at 10kN. The experimental cracking moment was calculated based on the following equation.

$$Mu = \frac{Pu*L}{4} \quad (1)$$

where, M_u is the cracking moment, L is the length of the specimen and P_u is the load at which the first crack is formed.

Figure 20 shows the comparison of the cracking and ultimate moment of beam 1 and beam 2.

Similar result was observed for the ultimate moment, where that for uncontaminated beam (Beam 1) was 20% higher compared to the contaminated beam (beam 2). This difference is due to the presence of oil in beam 2. The presence of oil have affected the bond strength between concrete and steel resulting in lower ultimate moment capacity of beam. The experimental evaluation of beam 1 and beam 2 shows a difference of 20.5%. The presence of oil reduces the bond between the concrete and steel which led to the earlier failure of beam 2. This behaviour was in a good agreement with the results from previous study conducted by King and Abousnina [38].

4. Data analysis and modelling

4.1 Prediction on compressive strength of concrete with oil contamination

Data analysis and modelling was conducted to develop simplified prediction equations for the mechanical properties of a concrete mix containing fine sand contaminated with light crude oil. The simulation data was analysed with a one-way repeated Analysis of Variance ANOVA [43] to confirm the significance of light crude oil in the modelling of compressive strength. The ANOVA results are shown in Table 4 for F-statistics and p-values. Parameters with $p < 0.01$ were considered to have a significant impact on the compressive strength. The analysis results indicate that the compressive strength was affected by each value of light crude oil as p-value was 2.19203×10^{-12}.

Table 4 ANOVA results for main and interaction effects

Source	*Sum of squares*	*Degree of freedom*	*Mean squares*	*F-statistics*	*p-values*
Light crude	934.217	5	186.8	326.5	2.19×10^{-12}

oil	

The relationship between compressive strength and light crude oil can be established from the ANOVA analysis. It was found that there was a polynomial relationship between the compressive strength and the level of light crude oil contamination. The rational model shown in Equation 2 was formulated to estimate the compressive strength as a function of crude oil, from a nonlinear regression analysis of the simulation data using MATLAB. The equation also shows the correlation coefficient (R^2) and the Root Mean Squared Error (*RMSE*) of the proposed model.

$$f'_{c(x)} = \begin{cases} f'_{cu} + 1.0x & 0 \leq X \leq 1.0 \quad \text{Adj. } R^2 = 1, \text{ RMSE} = 1.07 \\ f'_{cu} - 1.03x & 1.0 < X \leq 20.0 \quad \text{Adj. } R^2\ 0.99, \text{ RMSE} = 0.87 \end{cases} \qquad (2)$$

where $f'_{c(x)}$ is the predicted compressive strength containing fine sand with oil contamination, f'_{cu} is the average compressive strength of uncontaminated concrete, and x is the level of oil contamination in percentage. This model can be used to predict the compressive strength of concrete containing any percentages of light crude oil contamination up to 20%. This proposed empirical equation was validated with the experimental results. Figure 21 shows the resulting (f'_{cp}) scatter point plot of the predicted compressive strength (CS-predicted) against the experimentally measured compressive strength (CS-Experimental). As can be seen in Figure 21 that all points are located close to the line, which indicates the high accuracy (correlation coefficient of 99%) of the Equation 1.

Figure 21 Validation of the proposed equation of the compressive strength of concrete containing crude oil with simulation results

4.2 Relationship between the compressive strength and Splitting tensile strength of concrete

Splitting tensile strength is an important parameter to evaluate the shear resistance provided by concrete. The splitting tensile strength is generally greater than direct tensile strength. The Australian standard of concrete structures AS 3600 [44] proposed that the splitting tensile strength is 40% of the square root of compressive strength. Figure 22 plots the AS 3600 model and the splitting tensile strength obtained from this study, against compressive strength. For same compressive strength, it can be seen that the AS 3600 model underestimates the splitting tensile strength values which is predicted using the equation for conventional concrete. However, the relationship between tensile and compressive strength of concrete with oil-contaminated sand showed similar behaviour to conventional concrete. In both cases the tensile strength of concrete increases with the increasing compressive strength. The higher strength of concrete with fine sand contaminated with light crude oil makes it a potentially viable material for many civil engineering applications. The relationship between tensile (f_{ct}) and compressive (f_c) strength of the concrete with crude oil contamination can be expressed by the following equation.

$$f'_{ct} = 0.27f'_{c} + 1.03 \quad (3)$$

Figure 22: Tensile and compressive strength relationship

4.3 Prediction of Bond strength

Empirical Equations have been developed in Engineering, over time, following several experimental investigations in an effort to better understand various mechanisms. There are various bond strength models that have been developed by various researchers such as Zuo and Darwin [45] and Mohamed H. Harajli and Ahmad [46], etc. The development of bond strength relationship is mainly dependant on a number of key factors such as concrete cover, thickness, strength of concrete, diameter of steel bars, space between bars, splice lengths, rib ratio and shape [47]. These factors are important in understanding the behaviour of bond strength of deformed steel bars to concrete.

Wu and Zhao [47] undertook significant analysis of various bond strength and bond-slip models that were published in the last several decades. Their aim was to develop a unified bond strength and bond-slip models. Desnerck, et al. [48] also studied various bond strength prediction models of normal concrete during their study on self-compacting concrete. Based on the studies of both the authors, four bond strength models were chosen for this study. These four bond strength models were tested with the experimental compressive strength (f'_c) data to determine their predicted theoretical bond strength. This was plotted on the same graph as the experimental bond strength data as shown in Figure 23.

Table 5: shows four theoretical bond strength data calculated from the four different equations.

Model 1 * Wu and Zhao (2013) [47], Model 2 * Eligehuasen (1983) [49]

Model 3* Esfahani (2005) [50], Model 4 * Harajli (2004) [46]

Figure 23: shows the bond strength models plotted against percentage contamination level.

From Table 5 and Figure 23, after running the data through the four equations, it was found that the equation produced by Harajli (2004) (model 4), is the most reliably predicted bond strength up to 6% oil contaminated sand.

4.4 Prediction of flexural behaviour of beams

Data analysis and modelling was conducted to develop simplified prediction equations for the cracking and ultimate moment based on the experimental results. The developed equations will be used to predict the cracking moment and ultimate moment capacity for beams with different levels of oil contamination. As it can be seen in Figure 24, the cracking moment and ultimate moment capacity as a function of the compressive strength. Linear equations were developed to predict the cracking and ultimate moment capacity for different percentages of crude oil contaminations.

Figure 24: Developed equations of cracking and ultimate moment of uncontaminated beam (beam 1) and contaminated beam (beam 2).

Figure 25 shows the results of the predicted values of cracking and ultimate moment of all different crude oil contaminations. It can be seen that there is a linear relationship between the cracking and the ultimate moment and the compressive strength with different levels of light crude oil contamination.

where M_{crp} is the predicted cracking moment, M_{up} is the predicted ultimate moment, $f_{\prime c}$ is the compressive strength with different crude oil contaminations. This model can be used to predict the cracking and ultimate moment of different level of crude oil contaminations. This proposed empirical equation was validated with the experimental results

Figure 25: proposed equation of the cracking and ultimate moment of concrete containing crude oil

5. Conclusions

The physical, mechanical, and microstructure of concrete containing fine sand with different levels of light crude oil contamination (0, 1, 2, 6, 10 and 20%) were investigated. Moreover, the bond strength of steel reinforcement and the flexural behaviour of steel reinforced beams using concrete with 0% and 6% oil contamination was carried out. Simplified empirical equations were also proposed to reliably predict the mechanical properties of concrete containing oil contaminated sand. Based on the results, the following conclusions can be drawn from this study:

- The concrete density decreases as the oil content increases due to an increase in surface porosity. The surface wetness of the hardened concrete also increased with increasing levels of oil contamination.
- The compressive strength of concrete was enhanced at 1% oil contamination due to the sand reaching optimum cohesion as a result of oil binding sand particles. However, the concrete containing fine sand with 2% to 6% of light crude oil contamination exhibited up to 25% lower compressive strength than uncontaminated samples. Increasing the crude oil from 10% to 20% resulted in significantly lower strength than the uncontaminated concrete, due to surface saturation of aggregates which decreased the bond formation with the cement paste.
- The splitting tensile strength was enhanced by 7% at 1% of crude oil contaminations compared to uncontaminated samples. Higher than 1% oil contamination level, the tensile strength decreased as the sand became saturated with oil and the surface of the course aggregates was coated with oil hindering the physical bond formation between cement paste and aggregates.
- Oil contaminated sand up to 6% gives adequate bond strength similar to uncontaminated concrete while samples with 10% and 20% lost one third and three

quarter of its bond strength relative to uncontaminated respectively. This reduction of bond strength was due to lost chemical adhesion and frictional resistance caused by presence of high quantity of oil at high percentages.

- The maximum load that the contaminated beam (6%) could bear was 20% less than the uncontaminated beam. Furthermore, the initial crack and the yielding period of oil contaminated beam was at lower load and shorter period respectively compared to uncontaminated beam. However, the initial stiffness remains same for both the beams.

- SEM images showed that the full hydrated area is increased while the porosity decreased at 1% crude oil contamination, compared to uncontaminated concrete. At higher oil contamination levels (2% to 20%), the C-S-H gel decreased due to the higher amount of free water, which created more and bigger pores than the uncontaminated concrete.
- Simple empirical equations to predict the compressive strength of mortar and concrete containing oil contaminations were developed. Comparison between the experimental results and the predicted values for up to 20% oil contamination gave a 98% accuracy, indicating the reliability of the proposed equations.

Acknowledgements

The assistance by Zaffar Mohammed and Peter Mathew from USQ in conducting the test are acknowledged, the Endeavour Leadership Program Australia is also acknowledged.

References

[1] National Academy of Science, "Petroleum in the Marine Environment, ," National Academy Press, Washington, D.C.1975.

[2] H. Al-Sanad, W. Eid, and N. Ismael, "Geotechnical Properties of Oil-Contaminated Kuwaiti Sand," *Journal of Geotechnical Engineering,* vol. 121, no. 5, pp. 407-412, 1995.

[3] Mashalah Khamehchiyan, A. H. C. and, and M. Tajik, "The effects of crude oil contamination on geotechnical properties of Bushehr coastal soils in Iran," *IAEG,* p. 6, 2006.

[4] T. F. S. B. Products, "Strorage Tank Fire Protection-Leave Nothing to Chance," 2008.

[5] M. E. E. Survey, "Ras Lanuf Extinguished After Seven Days," *Middle east economic survey,* vol. 51, no. 35, p. 34, 2008.

[6] Z. Mohammed, "Bond behaviour of steel reinforcement to concrete with oil contaminated sand " BSc, Bachelor of Engineering Civil, USQ, USQ, Australia, 2015.

[7] E. Khosravi, H. Ghasemzadeh, M. R. Sabour, and H. Yazdani, "Geotechnical Properties of Gas Oil-Contaminated Kaolinite," *Engineering Geology,* vol. 166, pp. 11-16, 2013.

[8] R. Riser, "Remediation of petroleum contaminated soils: biological, physical & chemical processes," ed: United States: Lewis Publisher, 1998.

[9] J. Virkutyte, M. Sillanpää, and P. Latostenmaa, "Electrokinetic soil remediation — critical overview," *Science of The Total Environment,* vol. 289, no. 1–3, pp. 97-121, 4/22/ 2002.

[10] A. T. Yeung and Y.-Y. Gu, "A review on techniques to enhance electrochemical remediation of contaminated soils," *Journal of Hazardous Materials,* vol. 195, no. 0, pp. 11-29, 11/15/ 2011.

[11] A. A. Al-Rawas, A. W. Hago, and H. Al-Sarmi, "Effect of lime, cement and Sarooj (artificial pozzolan) on the swelling potential of an expansive soil from Oman," *Building and Environment*, vol. 40, no. 5, pp. 681-687, 5// 2005.
[12] W. O. Ajagbe, O. S. Omokehinde, G. A. Alade, and O. A. Agbede, "Effect of crude oil impacted sand on compressive strength of concrete," *Construction and Building Materials*, vol. 26, no. 1, pp. 9-12, 2012.
[13] R. A. Ahad and B. Ramzi, "Compressive And Tensile Strength Of Concrete Loaded And Soaked In Crude Oil," 2000.
[14] B. S. Hamad, A. A. Rteil, and M. El-Fadel, "Effect of used engine oil on properties of fresh and hardened concrete," *Construction and Building materials*, vol. 17, no. 5, pp. 311-318, 2003.
[15] V. M. Hebatpuria, H. A. Arafat, H. S. Rho, P. L. Bishop, N. G. Pinto, and R. C. Buchanan, "Immobilization of phenol in cement-based solidified/stabilized hazardous wastes using regenerated activated carbon: leaching studies," *Journal of hazardous materials*, vol. 70, no. 3, pp. 117-138, 1999.
[16] M. Cullinane, R. Bricka, and N. Francingues, "An assessment of materials that interfere with stabilization/solidification processes," in *Proceedings of the 13th Annual Research Symposium*, 1987, pp. 64-71.
[17] M. Almabrok, R. Mclaughlan, and K. Vessalas, "Characterisation of cement mortar containing oil-contaminated aggregates," 2013.
[18] M. H. Almabrok, R. McLaughlan, and K. Vessalas, "Investigation of oil solidification using direct immobilization method," presented at the Environmental Research Event 2011, North Stradbroke Island, QLD, 2011.
[19] H. Shahrabadi and D. Vafaei, "Effect of kerosene impacted sand on compressive strength of concrete in different exposure conditions. ," *Journal of Materials and Environmental Science, ,* vol. 6(9),, pp. 2665-2672, 2015.
[20] Attom M., Hawileh R., and Naser M., "Investigation on concrete compressive strength mixed with sand contaminated by crude oil products," *Construction and Building Materials*, vol. 47, pp. 99-103, 2013/10/01/ 2013.
[21] N. Shafiq, C. S. Choo, and M. H. Isa, "Effects of used engine oil on slump, compressive strength and oxygen permeability of normal and blended cement concrete," *Construction and Building Materials*, vol. 187, pp. 178-184, 2018/10/30/ 2018.
[22] R. Abousnina, A. Manalo, W. Lokuge, and Z. Zhang, "Effects of light crude oil contamination on the physical and mechanical properties of geopolymer cement mortar," *Cement and Concrete Composites*, vol. 90, pp. 136-149, 2018/07/01/ 2018.
[23] D. M. William, Jr., , *The Properties Petroleum Fluids, penn wells book Second Edition*. printed in USA, 1990.
[24] *Methods for sampling and testing aggregates - Particle size distribution - Sieving method*, 2009.
[25] *Methods of testing concrete - Preparing concrete mixes in the laboratory* 2014.
[26] C. Ltd. (2009). *C. Putoline HPX Fork & Suspension Oil* Available: http://www.championmotouk.com/product-info-t.php?Putoline-HPX-Fork-Suspension-Oil-pid10650.html
[27] SImetric. (2011). *specific gravity of liquids*. Available: http://www.simetric.co.uk/si_liquids.htm
[28] R. M. Abousnina, A. Manalo, and W. Lokuge, "Physical and Mechanical Properties of Cement Mortar Containing Fine Sand Contaminated with Light Crude Oil," *Procedia Engineering*, vol. 145, pp. 250-258, 2016.

[29] R. M. Abousnina, A. Manalo, W. Lokuge, and J. Shiau, "Oil Contaminated Sand: An Emerging and Sustainable Construction Material," *Procedia Engineering,* vol. 118, pp. 1119-1126, 2015.

[30] R. M. Abousnina, A. Manalo, J. Shiau, and W. Lokuge, "Effects of Light Crude Oil Contamination on the Physical and Mechanical Properties of Fine Sand," *Soil and Sediment Contamination: An International Journal,* vol. 24, no. 8, pp. 833-845, 2015/11/17 2015.

[31] *Methods of testing concrete - Preparing concrete mixes in the laboratory Standard Australia, Australia.*, 2014.

[32] R. C. Dorf, *The engineering handbook*. CRC Press, 2004.

[33] *Compressive strength tests concrete, mortar and grout specimens* 2014.

[34] *Determination of indirect tensile strength of concrete cylinders*, 2000.

[35] *Guide test methods for FRPs for reinforcing or strengthening concrete structures." ACI 440.03R-04, Farmington Hills, MI, ,* 2004.

[36] M. Almabrok, R. McLaughlan, and K. Vessalas, "Characterisation of cement mortar containing oil-contaminated aggregates," in *Australasian Conference On The Mechanics Of Structures And Materials*, 2013: CRC press/Balkema.

[37] F. W. Madderom and V. President, "Excess water can be a costly ingredient in concrete," *Concrete Construction,* 1980.

[38] A. D. Neuwald, "Water-to-Cement Ratio and Aggregate Moisture Corrections," National Precast Concrete Association, City Center Drive, Suite 200, Carmel, IN 46032, USA,2010.

[39] R. M. Abousnina, A. Manalo, J. Shiau, and W. Lokuge, "Effects of light crude oil contamination on the physical and mechanical properties of fine sand," *Soil and Sediment Contamination: An International Journal,* pp. 00-00, 2015.

[40] Y.-Y. Kim, K.-M. Lee, J.-W. Bang, and S.-J. Kwon, "Effect of W/C ratio on durability and porosity in cement mortar with constant cement amount," *Advances in Materials Science and Engineering,* vol. 2014, 2014.

[41] R. M. Abousnina, A. Manalo, W. Lokuge, and J. Shiau, "Oil Contaminated Sand: An Emerging and Sustainable Construction Material," *Procedia Engineering,* vol. 118, no. Supplement C, pp. 1119-1126, 2015/01/01/ 2015.

[42] O. I. George Abednego, Oba Achemie, Akpan Paul, Sarogoro Samuel, "Effects of crude oil contaminant on the engineering properties of concrete," *American Journal of Civil Engineering,* vol. 3, no. 5, pp. 178-182, 2015.

[43] R. G. Miller Jr, *Beyond ANOVA: basics of applied statistics*. CRC Press, 1997.

[44] *Concrete structures,* 2017.

[45] J. Zuo and D. Darwin, "Bond slip of high relative rib area bars under cyclic loading," *ACI Structural Journal,* Article vol. 97, no. 2, pp. 331-334, 2000.

[46] B. S. H. Mohamed H. Harajli and A. R. Ahmad, "Effect of Confinement on Bond Strength between Steel Bars and Concrete," *Structural Journal,* vol. 101, no. 5, 9/1/2004 2004.

[47] Y.-F. Wu and X.-M. Zhao, "Unified Bond Stress–Slip Model for Reinforced Concrete," *Journal of Structural Engineering,* vol. 139, no. 11, pp. 1951-1962, 2013.

[48] P. Desnerck, G. De Schutter, and L. Taerwe, "Bond behaviour of reinforcing bars in self-compacting concrete: experimental determination by using beam tests," *Materials and Structures,* journal article vol. 43, no. 1, pp. 53-62, December 01 2010.

[49] R. Eligehausen, Popov, E. P., and Bertero, V. V. (1983). "Local bondstress-slip relationships of deformed bars under generalized excitations: Experimental results and analytical model.'' EERC " *Earthquake Engrg. Res. Ctr., University of California, Berkeley, Richmond, Calif*, pp. 83-23,.

[50] M. R. Esfahani, M. R. Kianoush, and M. Lachemi, "Bond strength of glass fibre reinforced polymer reinforcing bars in normal and self-consolidating concrete," *Canadian Journal of Civil Engineering*, vol. 32, no. 3, pp. 553-560, 2005/06/01 2005.